

Fitts' index of difficulty predicts the $1/f$ structure of movement amplitude time series

Andrew B. Slifkin · Jeffrey R. Eder

Received: 8 August 2013 / Accepted: 7 January 2014 / Published online: 15 February 2014
© Springer-Verlag Berlin Heidelberg 2014

Abstract Studies using a variety of experimental tasks have established that when humans repeatedly produce an action, fluctuations in action output are highest at the lowest frequencies and fluctuation magnitude (power) systematically declines as frequency increases. Such time series structure is termed *pink noise*. However, the appearance of pink noise seems to be limited to tasks where action is executed in the *absence* of task-related feedback. A few studies have demonstrated that when action was executed in the *presence* of task-related feedback, power was evenly distributed across all spectral frequencies—i.e., *white noise* was revealed. Here, participants produced cyclical aiming movements under visual feedback conditions and we sought to determine whether variations of both the movement amplitude requirement (A) and the target width (W)—in the form of the index of difficulty [$ID = \log_2(2A/W)$]—would predict the structure of movement amplitude (MA) time series. There were two ID levels, and there was a small- and large-scale version of each ID: The A and W values of the large-scale version were twice those used for the small-scale version. Given that increases in ID are known to induce increased reliance on the available visual feedback, we predicted an ID-induced shift in MA time series structure from pink to white noise. Indeed, that is what we found. Further, there were no changes in MA structure when scale level changed within each ID level. Such scale invariance of MA time series structure reinforces the notion that MA structure depends on the combined influence of A and W .

Keywords Manual aiming · Index of difficulty · Fitts' law · Visual feedback · Time series structure · Pink noise · White noise

Introduction

In examinations of long time series of events, a commonly reported finding—across a range of physical, biological, and cognitive systems—is that fluctuations in system output are highest at the lowest frequencies with fluctuation amplitude declining as frequency increases. When spectral power (S) is the squared fluctuation amplitude at each frequency (f) [i.e., $S(f)$], $S(f)$ is proportional to the inverse of frequency ($1/f$), or $S(f) \propto 1/f^\beta$, where β specifies the degree of proportionality between $S(f)$ and $1/f$ (e.g., see Delignières et al. 2005, p. 455). If $\beta = 1$, then the scaling of $S(f):1/f$ is 1:1, and system output is said to have a *pink noise* structure (e.g., see Gilden 2001, Fig. 3). As seen in the simulated *pink noise* time series presented in the bottom panel of Fig. 1, a prominent low-frequency, high-amplitude oscillation is apparent and one may observe that as oscillation frequency increases, oscillation amplitude declines. In that case, the power spectrum would reveal systematic declines in power with increases in frequency, i.e., $\beta = 1$. In contrast, for the *white noise* time series shown in the top panel of Fig. 1, no regular oscillation can be seen and oscillation amplitude appears to be equal across all frequencies. That would give rise to a power spectrum where power is constant across the range of spectral frequencies, i.e., $\beta = 0$. In the current study, the value of β will be used to assess changes in the structure of movement amplitude (MA) time series as a function of Fitts' (1954) index of difficulty.

A recent, emerging view among some investigators of human movement control supports the idea that motor

A. B. Slifkin (✉) · J. R. Eder
Department of Psychology, Cleveland State University,
2121 Euclid Avenue, Cleveland, OH 44115, USA
e-mail: a.slifkin@csuohio.edu

SIMULATED TIME SERIES

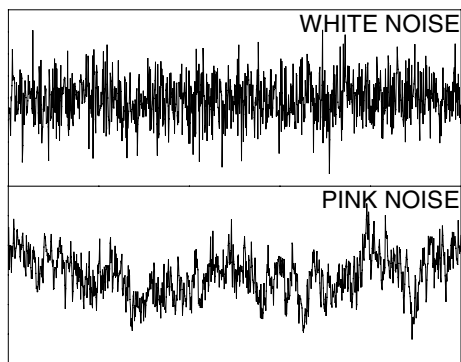


Fig. 1 Simulated white noise (*top panel*) and pink noise (*bottom panel*) time series

output power spectra should shift from pink noise to white noise whenever task demands require a shift from open-loop regulation (feedforward control)—based on the processing of internally stored information—to closed-loop regulation (feedback control)—based on the processing of external information (Wing et al. 2005; Diniz et al. 2011, p. 895; Slifkin and Eder 2012). For example, we recently reported a study where participants had to generate 1,000 consecutive cyclical aiming movements under each of a range of amplitude requirements under conditions of full visual feedback (Slifkin and Eder 2012). The resultant MA time series were submitted to spectral analysis and structure whitened with increases in the amplitude requirement. We attributed the shift in the structure of MA time series from pink to white noise to the extent to which closed-loop visual feedback processes were engaged during the execution of movement. That inference followed from the knowledge that under conditions of full visual feedback at small-amplitude requirements, MA is largely controlled by open-loop processes, but as amplitude requirements increase, MA control becomes increasingly governed by closed-loop visual feedback processes that correct for any error in the open-loop component and guide movement to the target (e.g., Elliott et al. 2001; Khan et al. 2006). In addition, we were able to account for our empirical results with a computer simulation where each simulated movement contained a primary open-loop component that contributed pink noise to MA time series and, if necessary, a secondary closed-loop visual feedback component that contributed white noise (Slifkin and Eder 2012, pp. 304–308): As the amplitude requirement increased in the simulation, maintenance of movement outcome success was dependent upon an increased contribution of the model's secondary closed-loop component, which resulted in the same pink-to-white noise shift as that seen in the empirical data.

Because only the amplitude requirement was varied in Slifkin and Eder (2012), while target width was held constant, we attributed the changes in MA structure to amplitude-requirement-induced variations in the engagement of closed-loop visual feedback processes. However, it could be that variations in target width or variations in the combination of movement amplitude requirement and target width could influence MA structure too (Slifkin and Eder 2012, see Footnote 3). In particular, in the current study, we test the combined influence of the amplitude requirement and target width on MA structure by varying the value of Fitts' index of difficulty [$ID = \log_2(2A/W)$], where the ID is expressed in bits of information, and where A is the movement amplitude requirement and W is the target width (Fitts 1954). The ID increases whenever A —the distance over which the effector needs to travel—is increased and/or W —the tolerance for endpoint error—is reduced. Note that the essence of the ID is the A -to- W ratio and not the absolute value of A or W alone. For example, if in one condition $A = 100$ mm and $W = 25$ mm but in another condition $A = 200$ mm and $W = 50$ mm, then the A -to- W ratio ($A/W = 4$) and ID ($ID = 3$ bits) would be the same for both conditions, despite the between-condition doubling of the absolute values of A and W . We will refer to a change in the values of A and W while ID remains constant as a change in *scale* (e.g., Slifkin and Grilli 2006).

In the current study, we examined the influence of changes in ID (2 and 5 bits) and changes in scale (small and large) within each level of ID on the structure of MA time series (see Fig. 2). Our first prediction is that increases in ID should result in a whitening of MA structure. It is already known that increases in A induce both increases in the engagement of closed-loop visual feedback processes (e.g., Elliott et al. 2001; Khan et al. 2006) and a whitening of MA structure (Slifkin and Eder 2012). In addition, as W declines—reducing the tolerance for endpoint error—engagement of closed-loop visual feedback processes increases (e.g., Annett et al. 1958; Buchanan et al. 2004) and there should be an increased whitening of MA structure too. Thus, if increases in A and reductions in W independently increase engagement of closed-loop visual feedback processes, then it follows that increases in ID should induce the same effect. Indeed, it is known that increases in ID result in increased engagement of closed-loop visual feedback processes (e.g., Crossman and Goodeve 1963/1983; Keele 1968; Meyer et al. 1988): For example, the increases in movement time (MT) that accompany increases in ID—i.e., Fitts' law or $MT = a + b[\log_2(2A/W)]$ —have been attributed to increased engagement of closed-loop visual feedback processes in MA control (e.g., see Keele 1968; Carlton 1992). Thus, again, in the current study, we predict an increased whitening of MA structure with increases in ID.

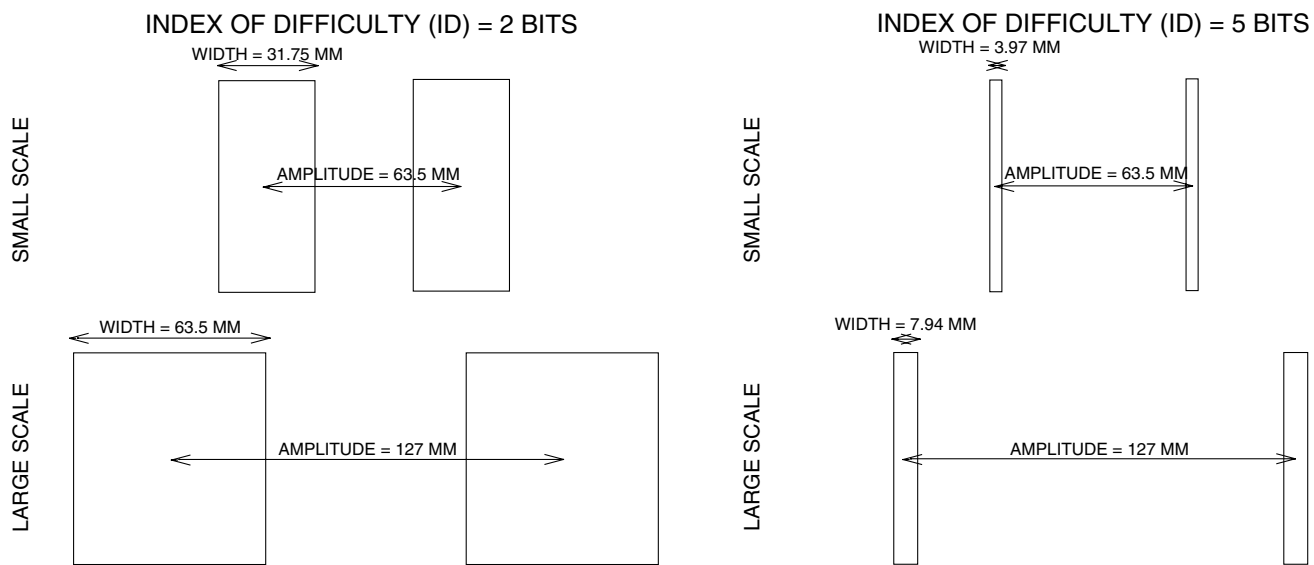


Fig. 2 Depictions of the four target displays. Fitts' (1954) equation for the index of difficulty (ID)— $ID = \log_2(2A/W)$ —was used to identify the amplitude requirement (A) and target width (W) values that provided two target displays with an ID value of 2 bits (*left half of figure*) and two target displays that had ID values of 5 bits (*right half of figure*). Within each ID level, there were two levels of target display scale. For ID 2, at the small-scale level, $A = 63.5$ mm and

$W = 31.75$ mm (*top left*), and at the large-scale level, $A = 127$ mm and $W = 63.5$ mm (*bottom left*). For ID 5, at the small-scale level, $A = 63.5$ mm and $W = 3.97$ mm (*top right*), and at the large-scale level, $A = 127$ mm and $W = 7.94$ mm (*bottom right*). Thus, as ID increases within a scale level, A is constant and W shrinks. However, within an ID level, both A and W double from the small-scale level to the large-scale level

A second prediction is that MA structure should be the same when both A and W values change but ID is constant, i.e., when there is a change in scale within an ID level. In the current experiment, as scale increases within an ID level, the values of A and W double (see Fig. 2). In that case, Fitts' law would predict common MTs—i.e., *scale invariance*—and it follows that there would be common engagement of closed-loop visual feedback processes. Therefore, there should be scale invariance for MA structure too. If both of our predictions are correct, then it would appear that the more parsimonious predictor of MA structure is ID, and not the absolute values of A or W alone.

Method

Participants

Sixteen healthy, young individuals, eight of whom were female, served as participants. The mean age of all participants was 23.75 (SD = 3.84), and all reported that they were right-hand dominant, had no prior history of neurological disease or damage, and had normal or corrected-to-normal vision. They responded to advertisements for healthy right-hand dominant volunteers between the ages of 18 and 30. The advertisements were flyers posted throughout the university. Each participant provided informed consent that was approved by the local institutional review

board. Upon completion of the experiment, they received a \$10.00 payment.

Apparatus

Movements were made on a 304.80 by 457.20 mm graphics tablet (Wacom Intuos2) using its cordless mouse (Wacom Intuos2 4D Mouse), and target displays were viewed on a 469.90 mm flat screen LCD video monitor (Acer X183H) with a refresh rate of 75 Hz and viewable dimensions of 230 mm in height by 430 mm in width. The graphics tablet was placed on a tabletop with a height of 742.95 mm, and the video monitor was placed on a stand that, in turn, was placed on the tabletop. (Placing the video monitor on the stand raised the height of the video monitor by 234.95 mm so that the center of the video monitor was at eye level for the typical participant.) The tablet was placed directly in front of the video monitor, and when a participant was seated at the table, their body midline was aligned with the midline of the tablet and monitor. Participants were allowed to adjust the chair to a comfortable height and distance from the table; the approximate distance from participants' eyes to the video monitor was 660.40 mm.

Procedure

Customized software ran the experimental contingencies and presented the target displays. Each target display

consisted of two targets that were equidistant from the center of the monitor. The targets appeared as thin, white rectangular outlines overlaying a black background. Target height was always set at 139.70 mm. As shown in Fig. 2, there were four target display conditions where each had a unique combination of A and W values. Using Fitts' (1954) equation for the index of difficulty (ID)— $ID = \log_2(2A/W)$ —we created two target displays that had an ID value of 2 bits and two target displays that had an ID value of 5 bits. The two target displays within each ID level represented two levels of scale. For ID 2, at the small-scale level, $A = 63.5$ mm and $W = 31.75$ mm (see Fig. 2, top left), and at the large-scale level, $A = 127$ mm and $W = 63.5$ mm (see Fig. 2, bottom left). For ID 5, at the small-scale level, $A = 63.5$ mm and $W = 3.97$ mm (see Fig. 2, top right), and at the large-scale level, $A = 127$ mm and $W = 7.94$ mm (see Fig. 2, bottom right). Thus, as ID increases within a scale level, A is constant and W shrinks. However, within an ID level, both A and W double from the small-scale level to the large-scale level.

During each condition, a single target display was presented and 999 consecutive movements were completed. During that time, a cursor was continuously displayed on the video monitor. The x -dimension control-to-display mapping was 1:1 such that a unit of mouse movement along the x -dimension of the graphics tablet translated to a unit of cursor movement along the x -dimension of the video display. The y -dimension control-to-display gain was 1.33:1.00 such that a unit of mouse movement along the y -dimension of the graphics tablet resulted in 0.75 units of cursor movement along the y -dimension of the video display. All data presented in this report came from the x -dimension of movement. Throughout each movement, data acquisition occurred every 15 or 16 ms ($M \approx 15.5$ ms), which translates to instantaneous acquisition rates of either 66.67 or 62.50 Hz ($M \approx 64.52$ Hz), respectively. The spatial resolution of each sample was 0.1 mm.

At the start of the experimental session, the experimenter demonstrated the movement task and concurrently delivered the task instructions. Participants were instructed that white crosshairs would serve as a *cursor* and its position on the video monitor would correspond to the position of the mouse on the graphics tablet. At the start of each movement condition, a white *marker*, also in the form of crosshairs, would appear in the center of the left target. Participants were told that the marker crosshairs identified the currently active target; however it was emphasized that a target hit would register if the cursor crosshairs “landed” anywhere within the active target region at the time of a mouse button press. In contrast, any button press occurring when the cursor crosshairs were outside of the target would be classified as a target miss and would be accompanied by a “beep” sounded by the computer. At the time of either a

target hit or a miss, the marker crosshairs changed location to the opposite target, and participants were instructed that they should move to that target and produce a button press when the cursor was in that target region. They were told to continue the sequence of back and forth movements until the target display disappeared from the screen. That event signaled the end of the sequence of 999 movements. Participants were told to be as fast and as accurate as possible in making their movements and that the instruction to be fast was of equal importance to the instruction to be accurate.

Following delivery of the instructions, participants practiced 49 movements under each target display condition. As during the experiment itself, the order of each participant's four practice conditions was randomized, with the exception that the consecutive administration of the two ID 5 conditions was not allowed. (That restriction on randomization was imposed to limit the buildup of fatigue that might accompany performance on consecutive ID 5 conditions.) At the end of each experimental condition, participants were allowed to rest as long as they needed. The total session duration was about 1 h, and the room lights were extinguished while the task was performed. Thus, the only task-related visual information available to participants was what was presented on the video screen, viz., the cursor and target displays. In addition, participants wore sound-attenuating earmuffs during experimental trials in order to minimize the potential influence of sound extraneous to the experiment. The volume of the computer-generated error “beep” was adjusted so participants could hear it through the ear muffs.

Experimental design and data analyses

General data processing

Movement amplitude was defined as the distance along the movement x -axis from the location of the mouse click that terminated movement at the previous target to the location of the mouse click that terminated movement at the current target. The time between those mouse clicks was the movement time (MT). The initial 99 movements of each time series were not analyzed, thereby excluding warm-up effects that may have been present during the initial portion of the performance time series. The remaining 900 movements were submitted to data analyses.

Mean movement time

While analysis of MA structure was the main focus of the current report, we also present an analysis of mean MT. The analysis of MT can provide information about the extent to which closed-loop visual feedback processes were engaged in the control of MA. That is, under instructions

to maximize speed and accuracy, increases in MT beyond a minimum value (e.g., ≈ 200 ms) correlate with increased engagement of closed-loop visual feedback processes (e.g., Meyer et al. 1988; Elliott et al. 2001, 2010). If increases in movement difficulty (ID) resulted in whitening of MA time series, then parallel increases in MT would provide evidence that such whitening arose from the engagement of closed-loop visual feedback processes. Fitts' law predicts, first, increases in MT with increases in ID, and, second, common MTs across scale levels within an ID level, i.e., scale invariance. Thus, with common MTs across scale levels within an ID level, the amount of visual feedback processing should be the same and the same MA structure should emerge too. Mean MT was calculated for each participant's movement time series under each of the four unique conditions. Then, a two-way ID (2) by scale (2) repeated-measures ANOVA was used to test the reliability of change in the group-mean MT across ID and scale levels.

Spectral analyses

Prior to spectral analysis, each 900-point MA time series was linearly detrended (e.g., Gildea 2001). The detrending involved calculating the best-fitting linear regression for each time series and obtaining the time series residuals, i.e., the difference between each time series value and the value predicted by the regression equation. That process removed the mean and any overall linear trend in the time series, but, otherwise, preserved the original time series structure. Then, the power spectral density for each residual MA time series was calculated in MATLAB v.7.1 using Welch's averaged, modified periodogram method, i.e., MATLAB's *pwelch* function. We chose *pwelch* parameter values that allowed each 900-point series to be divided into four non-overlapping segments of 225 data points. [In particular, the *pwelch* parameter values were (a) window = 225, (b) noverlap = 0, (c) nfft = 225, and (d) fs = 1.] Next, each 225-point segment was multiplied by a Hamming window followed by the calculation of the power spectral density of each segment. Finally, the four power spectral densities were averaged. The resultant average power spectrum from each time series was divided into 112 bins of equal width where the frequencies associated with the upper limits of the lowest and highest frequency bins were, respectively, 0.0044 and 0.4978 cycles per movement (Hz), which translated to 225 and 2.0089 movements per cycle for the upper limits of the lowest and highest frequency bins, respectively. Each frequency bin spanned a 0.0044 Hz range. The amount of power in each frequency bin was related to the magnitude of the MA oscillations within the frequency range specified by that frequency bin.

Our main measure of MA structure was an estimate of β from the power spectrum. This involved a \log_{10} transformation of both the spectral power and frequency of each participant's power spectrum. Then, linear regression— $y = bx + a$ —was used to describe changes in \log_{10} power as a function of \log_{10} frequency. In that case, the negative of b is equivalent to β in the equation for the power function $S(f) = 1/f^\beta$. In other words, if the linear regression b has a value of -1 , then the power function β has a value of 1. The linear regression equation spanned the lowest frequency bin, which had an upper limit of 0.0044 Hz—or -2.356 Hz after the \log_{10} transformation—to the frequency bin with an upper limit of 0.0978 Hz—or -1.0098 Hz after the \log_{10} transformation (see Footnote 6 in Slifkin and Eder 2012, for more information about selection of the -1.0098 cutoff). A two-way ID (2) by scale (2) repeated-measures ANOVA was used to examine changes in the group-mean β as a function of ID and scale level. All results reported as “significant” had P values less than 0.05.

Results

Figure 3 provides examples of time series collected in the current study; they illustrate a change in MA structure across ID levels. The example time series are composed of the MA residuals collected from a single participant under the large-scale target display conditions of ID 2 (top panel) and ID 5 (bottom panel). At ID 2, there appear to be pronounced wavelike oscillations at low frequencies and lower-amplitude oscillations at higher frequencies. On the other hand, at ID 5, the prominence of low-frequency wavelike oscillations appears to be attenuated, and oscillation amplitude appears more even across a broader range of frequencies. The value of β based on the ID 2 MA time series was 0.42, while the value of β based on the ID 5 MA time series was -0.04 . Thus, Fig. 3 demonstrates an ID-induced shift in structure from a value in the vicinity of pink noise, at ID 2, to a value essentially equivalent to white noise, at ID 5. While the current empirical results focus on further analyses of the MA power spectrum as a function of ID and scale, prior to that presentation, we provide an analysis of the group-mean MT.

Mean movement time

Figure 4 shows changes in the group-mean MT as a function of ID and scale. When averaged across scale levels, the group-mean MT increased from 426.67 ms at ID 2 to 896.10 ms at ID 5. The increase in the group-mean MT with increases in ID was significant, $F(1, 15) = 693.27$, $P < 0.001$. At ID 2, the group-mean MT under the large-scale requirement was elevated by 34.66 ms over the MT at

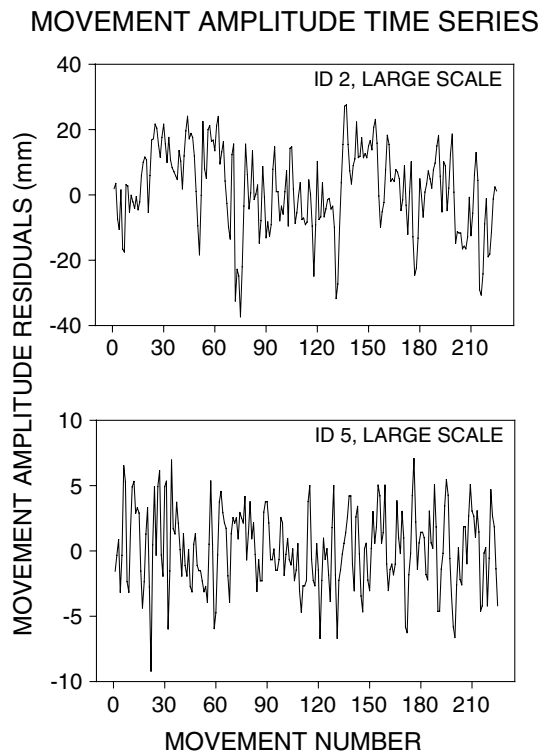


Fig. 3 Example segments of movement amplitude (MA) time series during cyclical aiming at the large-scale index of difficulty of 2 bits (ID 2) (see *top panel*) and 5 bits (ID 5) (see *bottom panel*). Both examples were taken from the same participant, and each example represents a segment of 225 consecutive movements taken from a linearly detrended time series that contained a total of 900 movements. The detrending procedure returns the deviations (residuals) from the best-fitting linear regression equation. The structure of those time series was captured by β values derived from power spectra computed using the same MATLAB v.7.1 *pwelch* parameter values applied to all spectral analyses described in this study (see “[Method](#)” section). At the ID 2 (*top panel*) and ID 5 (*bottom panel*) conditions, β equaled 0.42 and -0.04 , respectively. While those β values were based on power spectra of single segments of 225 data points, for all other time series in this study, overall power spectra were obtained by averaging across four individual power spectra, one for each 225 data-point segment within a 900 data-point time series (see “[Method](#)” section)

the small-scale requirement; at ID 5, the group-mean MT was essentially identical at the different scale levels—the between-scale difference in the group-mean MT was less than 1 ms. Both the scale effect and the ID by scale interaction were absent. Although we examined only two ID levels and two levels of scale within each ID level, the current results do follow the predictions of Fitts’ law: MT should increase with ID, and MT should be constant across variations in scale within a level of ID, i.e., scale invariance should be observed. The linear regression equation describing changes in the group-mean MT as a function of ID was $y = 156.477x + 113.715$, $r^2 = 0.997$, or, as restated in the form of Fitts’ law, $MT = 113.715 + 156.477[\log_2(2A/W)]$, $r^2 = 0.997$.

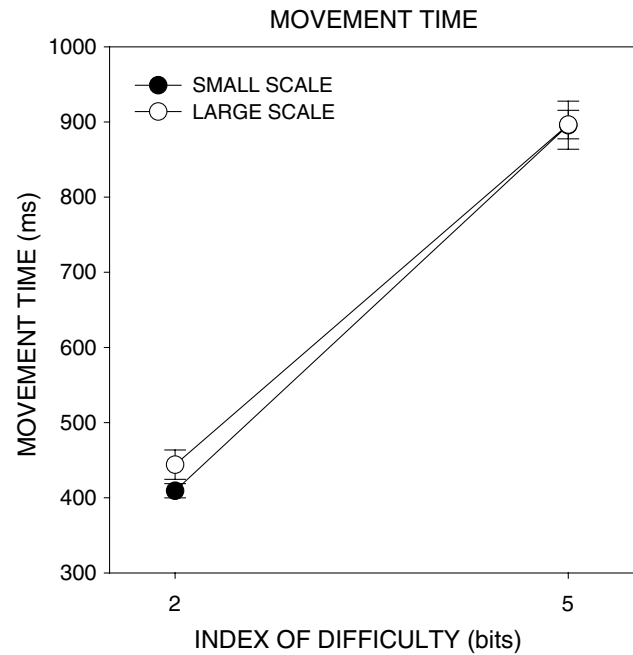


Fig. 4 Changes in the group-mean movement time (MT) as a function of the index of difficulty (ID) and scale level. Each data point represents the group-mean MT based on an across-participant average at each ID and scale level. The *error bars* around group-mean data points represent ± 1 SEM

Given that MTs under all requirements were longer than typical estimates of minimum visual processing times (e.g., ≈ 200 ms), it would appear that the opportunity to engage visual feedback existed under all conditions (e.g., Keele and Posner 1968; Keele 1968; Carlton 1992), and the engagement of visual feedback processes increased as ID increased. Thus, if there was a whitening of MA time series structure as ID increased, then the results of the current analysis of MT would support the notion that such whitening was mediated by closed-loop visual feedback processes.

Spectral analyses

Figure 5 shows the group-mean power spectrum at each ID and each scale level. For each spectrum, linear regression equations provided a nice description of changes in \log_{10} power as a function of \log_{10} frequency. At least two other general observations can be made: First, the overall level of power was reduced with increases in ID. In other words, the magnitude of MA variability—as would be reflected by a descriptive statistic like the within-subject standard deviation—was reduced with increases in ID. That result can be understood as it was under both ID 2 target displays that the larger W values permitted more space in which MA values could vary. Likewise,

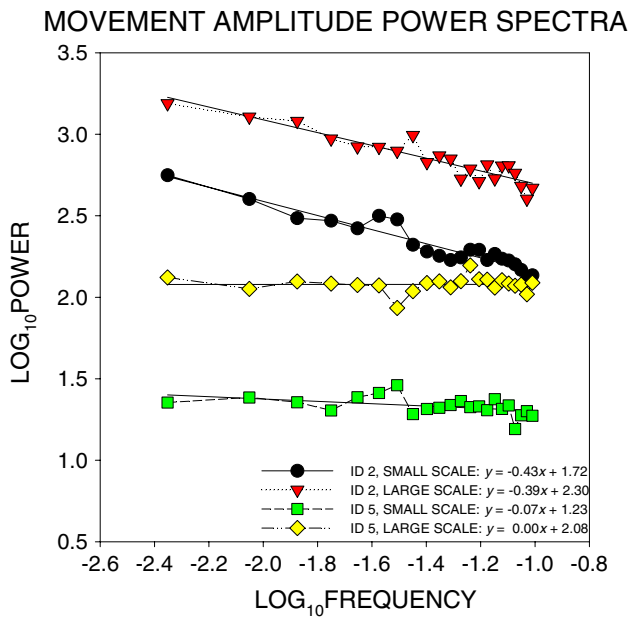


Fig. 5 Changes in the group-mean power spectrum across index of difficulty (ID) and scale conditions. Each data point within each spectrum represents the across-participant average of \log_{10} power within a given \log_{10} frequency bin. The negative of the slope ($-b$) of the linear regression equation— $y = bx + a$ —fit to each group-mean power spectrum was equivalent to the exponent (β) of the power function— $y = 1/x^\beta$ —which was taken as the measure of time series structure, i.e., if $b = -1$, then $\beta = 1$

within each ID level, the reduced elevations of the power spectrum as scale was reduced could be attributed to the reduction in W . Second, and more importantly, the slopes of the regression equations (b) are quite similar and parallel across scale levels within each ID level. The value of b clearly shifts from negative values at ID 2 and flattens to near-zero values at ID 5. In particular, when averaged across scale levels, the b values were -0.41 and -0.03 at ID 2 and ID 5, respectively. Thus, the distribution of power leaned toward pink noise at ID 2 and whitened at ID 5.

The group-mean β coefficients are plotted in Fig. 6. That pattern of results mirrors the slopes of the regression equations based on the group-mean power spectra shown in Fig. 5. As ID increased, β was reduced toward a value of 0. The reliability of that reduction was confirmed by a significant ID effect from the two-way ANOVA, $F(1, 15) = 34.97, P < 0.001$. The small-scale β was elevated over the large-scale β within each ID. However, those differences were small and there was not a scale effect. In addition, a reliable ID by scale interaction was absent. Thus, it would appear that the ID is predictive of MA structure: There were reliable decreases in the value of β with increases in ID and β values were scale invariant. Last, linear regression showed that variations in ID were

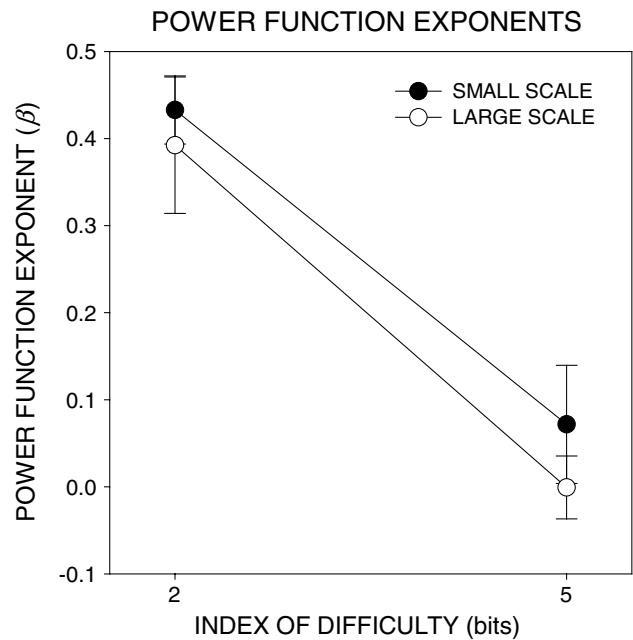


Fig. 6 Changes in the group-mean β as a function of the index of difficulty (ID) and scale level. β is the exponent of a power function— $y = 1/x^\beta$ —and the power function was fit to each participant’s power spectrum at each ID and scale level. Then, each group-mean β value was calculated by averaging across the individual-participant β s at a given ID and scale level. The error bars around group-mean data points represent ± 1 SEM

highly predictive of variations in the group-mean β , $y = -0.128x + 0.664, r^2 = 0.976$.¹

Discussion

We recently demonstrated a whitening of MA time series structure when A increased, but W was held constant

¹ In addition to using β from the power spectrum, we also undertook an analysis of α from detrended fluctuation analysis (DFA) (see Peng et al. 1995). If $\alpha = 1$, then the time series has a pink-noise structure, and if $\alpha = 0.5$, then the time series has a white noise structure. If the pattern of results for α matched the pattern of results for β , then that would validate the current analysis based on β alone. To that end, we calculated α values for the same data used to calculate β and we also submitted that data to a two-way ID (2) by scale (2) repeated-measures ANOVA. The results revealed a significant ID effect with a reduction in α from ID 2 ($M = 0.71, SEM = 0.03$) to ID 5 ($M = 0.56, SEM = 0.02$), $F(1, 15) = 34.18, P < 0.001$. Both the scale effect, $F(1, 15) = 0.102, P = 0.75$, and the ID by scale interaction, $F(1, 15) = 0.96, P = 0.34$, were absent. Thus, as seen in the analysis of β , for α there was only an ID effect reflecting a whitening of MA time series as ID increased. In addition, variations in the group-mean β values were highly predictive of variations in the group-mean α values, $y = 0.398x + 0.546, r^2 = 0.945$. The correspondence between α and β has been observed in prior studies of MA time series structure (Miyazaki et al. 2004, see Table 1; Slifkin and Eder 2012, see Footnote 7).

(Slifkin and Eder 2012). Those changes were attributed to increases in A , but it could be that the combined influence of A and W serves as a more powerful predictor of MA structure. Therefore, in the current experiment, we examined the combined influence of A and W —in the form of the ID—on changes in MA structure. In addition to varying ID, we varied target display scale, where the small-scale target displays had A and W values that were half the A and W values of the large-scale target displays. It was predicted that MA structure should whiten with increases in ID, but MA structure should remain constant across scale levels within each ID level. Because of the large changes in both A and W across scale levels within each ID level, a finding of scale invariance for MA structure would highlight the value of the combined influence of A and W in predicting MA structure, and not their independent and absolute values. Indeed, we found, first, that as ID increased, MA structure whitened, but, second, changes in scale at each ID level resulted in constancy of MA structure, i.e., scale invariance.² Thus, ID not only predicts variation in MT (Fig. 4)—as in Fitts' law—but also predicts variations in MA structure (Fig. 6). Again, according to the current results, it is the combined influence of A and W —in the form of the A -to- W ratio or the ID—that has greater power in predicting MA structure, as opposed to A or W considered alone. The remainder of the Discussion will be a review of the information processes that might be involved in the ID-induced changes in MA structure we observed.

What motor control information processes would give rise to the whitening of MA structure with increases in ID? It is already known that increases in A induce both increases in the engagement of closed-loop visual feedback processes (e.g., Elliott et al. 2001; Khan et al. 2006) and a whitening of MA structure (Slifkin and Eder 2012). In addition, as W declines—reducing the tolerance for endpoint error—engagement of closed-loop visual feedback processes increases (e.g., Annett et al. 1958; Buchanan et al. 2004). Thus, if increases in A and reductions in W independently increased engagement of closed-loop visual feedback processes, then it follows that increases in

ID should induce the same effect. Indeed, there is good evidence—through analyses of trajectory submovements and manipulation of visual feedback—that increases in ID induce increased engagement of closed-loop visual feedback processes (e.g., Crossman and Goodeve 1963/1983; Keele 1968; Keele and Posner 1968; Meyer et al. 1988). In addition, the increases in MT that accompany increases in ID—i.e., Fitts' law: $MT = a + b[\log_2(2A/W)]$ —have been attributed to increased engagement of closed-loop visual feedback processes in MA control (e.g., see Keele and Posner 1968; Keele 1968; Carlton 1992). That follows because the processing and use of feedback in the control of movement takes time; thus, with more feedback being processed, MT should lengthen. In the current experiment, we found that variations in MT followed Fitts' law (Fig. 4): MT increased with ID and MT remained constant across scale levels. In particular, MTs more than doubled from an across-scale-level average of about 425 ms at ID 2 to about 900 ms at ID 5: MTs lengthened to values several times longer than typical estimates of minimum visual processing times (e.g., ≈ 200 ms; Keele and Posner 1968; Carlton 1992). Thus, the results of the current analysis of MT support the notion that the ID-induced whitening of MA structure was mediated by closed-loop visual feedback processes operating during movement execution.

There was a very close correspondence between changes in MT and changes in β in the current results. First, β is predicted by ID just as MT was predicted by ID (cf. Figs. 4, 6): Thus, just as Fitts' law is $MT = a + b[\log_2(2A/W)]$, the current results suggest that $\beta = a + b[\log_2(2A/W)]$. Second, MT values are highly predictive of β values, and vice versa. The very strong relationship between MT and β is illustrated by a regression equation that predicts the group-mean β s (Fig. 6) based on the group-mean MTs (Fig. 4), $y = -0.0008x + 0.7561$, $r^2 = 0.981$. Given that MT and β are similarly predicted by ID, and β and MT are strongly associated, one may ask how MT and β are similar or different in terms of the information processes they reflect: As previously discussed, variations in MT are thought to reflect variation in the engagement of closed-loop visual feedback processes that act *within* a movement (e.g., Keele and Posner 1968; Carlton 1992), whereas β reflects the relations *between* or *among* MA values in long sequences of action. As more time is used in the closed-loop control of movement and MT increases, MA values become decorrelated and β values are reduced. That occurs because online visual feedback is tailored to the error correction needs of individual movements, and such within-movement adjustment breaks up the underlying pink noise structure contributed by the initial open-loop component of movement. In other words, the whitening of MA structure is a product of the superimposition of closed-loop processes upon preexisting open-loop processes.

² In a recent study by Wijnants et al. (2012), participants performed in a cyclical aiming task and—although it was not the primary goal of the study—the authors examined the influence of ID [3 bits ($A = 80$ mm, $W = 20$ mm), 6.9 bits ($A = 240$ mm, $W = 4$ mm)] on MA time series structure (Wijnants et al. 2012, Table 1, p. 11). Their “fractal dimension” measure of MA structure—which is related to β from the power spectrum and α from detrended fluctuation analysis—showed a slight, non-significant tendency toward increased MA time series whitening with increases in ID. In contrast, in the current study, there was significant MA time series whitening with increases in ID. The between-study difference in results might have been influenced by a number of differences between the Wijnants et al. (2012) study and the current study. A review of those differences is beyond the scope of the current report.

The view that the expression of long-range dependencies contributed by initial open-loop processes is degraded by the superimposition of closed-loop processes receives support from investigators who calculated β for time series based on either the amplitude at (Miyazaki et al. 2001) or the time to (Valdez and Amazeen 2008, 2009) various kinematic markers within movements made under full visual feedback and under high-ID conditions.³ First, in a discrete aiming task performed under instructions for movement speed and accuracy, Miyazaki et al. (2001) showed long-range dependencies for the amplitude at peak acceleration and the amplitude at peak velocity—both occurring early in the movement—but those dependencies were absent for MA—occurring at movement termination. Second, in discrete aiming tasks performed at comfortable speeds, Valdez and Amazeen (2008, 2009) showed that long-range dependencies were highest for the time to peak velocity and were reduced for MT—the time to the movement termination. To the extent that the processes regulating temporal variation of movement are the same as those regulating spatial variation of movement, the results from both sets of investigators (Miyazaki et al. 2001; Valdez and Amazeen 2008, 2009) are consonant with the current view that it is the superimposition of closed-loop feedback processes upon initial, open-loop processes that causes a whitening of MA structure. While Miyazaki et al. (2001, p. 176) entertained the possibility that an error correction process might be responsible for the dissipation of long-range dependencies at movement end, Valdez and Amazeen (2008, 2009) proposed that the heightened long-range dependencies at peak velocity were the result of the coordination or intermingling of “planning” (open-loop processes) and “control” (closed-loop processes). However, it is our view that long-range dependencies—which are a reflection of open-loop processes—can only be degraded, and not boosted, by the addition of closed-loop processes; closed-loop processes only whiten motor output and attenuate its long-range dependencies (see “Introduction” section; Slifkin and Eder 2012, pp. 304–308).

Other recent studies using targeted aiming tasks have proposed that the spatial structure of motor output time series whitens as a result of closed-loop feedback processes (van Beers 2009; van Beers et al. 2013). However, in those studies, the opportunity to process visual feedback during

movement execution was precluded and participants could only view movement outcome relative to the target at movement termination (terminal feedback). Thus, *within-movement* corrections would be minimized and adjustment in movement plans would occur following movement termination with a feedforward implementation of the updated plans occurring upon subsequent movement initiation. In addition, such *between-movement* processing of terminal feedback might have been encouraged by the use of a discrete-trials movement paradigm in those studies (van Beers 2009; van Beers et al. 2013). In such tasks, a delay is imposed between the end of one movement and the start of the next and that “space” might allow for more complete processing of the terminal feedback. In contrast, in the current study, participants had the opportunity to process visual feedback within each movement and there was less opportunity to process feedback at the end of movement: Participants were instructed to be as fast and accurate as possible while performing a cyclical aiming task, and there were no experimenter-imposed time intervals between movements. In such cases, closed-loop visual feedback processes should operate within movements instead of between movements (e.g., see Slifkin and Eder 2012, Footnote 9). In sum, although the degree of within- or between-movement feedback processing may be task dependent, both types of feedback processing appear to result in a whitening of the spatial structure of motor output time series.⁴

In conclusion, the results of the current study indicate that it is the combination of *A* and *W* together—in the form of the ID—that serves as an improved predictor of MA structure, as opposed to *A* or *W* alone. In fact, ID appears to predict β values with the same accuracy as MT, i.e., variations of β can be derived from Fitts’ law. We hypothesize that what underlies the ID-induced variations in MA structure is the extent to which open-loop versus closed-loop information processes are engaged. The lengthening of MT reflects an increased engagement of closed-loop

³ In Miyazaki et al. (2001) the ID level was 4.3 bits (see Footnote 8, Slifkin and Eder 2012). In Valdez and Amazeen (2008), participants had to move a handheld cylinder over different levels of *A* (400, 500, 600, 700 mm) and although the target *W* value was not reported it presumably had the same diameter as that of the cylinder, which was 45 mm (Valdez and Amazeen 2008, p. 305). In that case—according to the equation $ID = \log_2(2A/W)$ —the IDs would have ranged from 4.15 to 4.96 bits. In Valdez and Amazeen (2009), participants performed under conditions of either 3.90 or 4.90 bits.

⁴ In another recent study, using a task that incorporates features of tetherball and skittles (bowling), participants were required to throw and release a virtual ball so that it moved around a pole toward a target located about 180° from the throwing position (Abe and Sternad 2013). Participants performed extended discrete-trials sequences of the task and on each trial a measure of spatial error was recorded. The results appear to reflect an increased whitening of spatial structure that could be related to increased engagement of visual feedback. However, it is difficult to say whether the feedback was used within or between movements: Participants could see movement of the ball throughout each trial, but could only use visual feedback for online, within-movement control during the initial throwing phase; on the other hand, any feedback gained between ball release and trial termination could only be used for between-movement adjustments of a subsequent throw.

processes that are superimposed upon the underlying, pre-existing open-loop processes: Open-loop processes are expressed as long-range correlations in MA time series, but those correlations are degraded by the implementation of closed-loop error correction processes that act within and toward the end of movement. That view is consonant with an emerging, general view that when system output is primarily under internal control, pink noise is the product, but when systems rely on the processing of external information for their regulation, white noise is the product (Wing et al. 2005; Diniz et al. 2011, p. 895; Slifkin and Eder 2012). Last, among approaches that attempt to account for $1/f^\beta$ processes, the current approach represents a domain-dependent, *mechanistic* approach (e.g., for a brief review, see Slifkin and Eder 2012, p. 309): In the current study, we explained the $1/f^\beta$ structure of MA time series—unfolding over a long time scale—in terms of the degree of engagement of closed-loop visual feedback—a local, specific motor control mechanism acting over a short time scale. In contrast, those taking a *nomothetic* approach explain $1/f^\beta$ phenomena in terms of domain-independent, generic processes (e.g., self-organized criticality, cascade dynamics) that can be applied to a wide range of systems; such models do not require the identification of specific information-processing mechanisms. While the relative value of the mechanistic and nomothetic approaches has been debated, another view is that both approaches are valuable and complementary (e.g., Diniz et al. 2011).

Acknowledgments Partial support for this research was provided by a Cleveland State University Summer 2012 Engaged Learning/Creative Achievement Award made to Andrew B. Slifkin. The authors are grateful to Patrick Byrne for his assistance with data collection.

References

- Abe MO, Sternad D (2013) Directionality in distribution and temporal structure of variability in skill acquisition. *Front Hum Neurosci* 7:1–15
- Annett S, Golby CW, Kay H (1958) The measurement of elements in an assembly task: the information output of the human motor system. *Q J Exp Psychol* 10:1–11
- Buchanan JJ, Park JH, Shea CH (2004) Systematic scaling of target width: dynamics, planning, and feedback. *Neurosci Lett* 367:317–322
- Carlton LG (1992) Visual processing time and the control of movement. In: Proteau L, Elliott D (eds) *Vision and motor control*. North-Holland, Amsterdam, pp 3–31
- Crossman ERFW, Goodeve PJ (1963/1983) Feedback control of hand-movement and Fitts' Law. *Q J Exp Psychol* 35A:251–278
- Delignières D, Torre K, Lemoine L (2005) Methodological issues in the application of monofractal analyses in psychological and behavioral research. *Nonlinear Dyn Psychol Life Sci* 9:451–477
- Diniz A, Wijnants ML, Torre K, Barreiros J, Crato N, Bosman AM, Hasselman F, Cox RF, Van Orden GC, Delignières D (2011) Contemporary theories of $1/f$ noise in motor control. *Hum Mov Sci* 30:889–905
- Elliott D, Helsen WF, Chua R (2001) A century later: Woodworth's two-component model of goal-directed aiming. *Psychol Bull* 127:342–357
- Elliott D, Hansen S, Grierson LEM, Lyons L, Bennett SJ, Hayes SJ (2010) Goal-directed aiming: two components but multiple processes. *Psychol Bull* 136:1023–1044
- Fitts PM (1954) The information capacity of the human motor system in controlling the amplitude of movement. *J Exp Psychol* 47:381–391
- Gilden DL (2001) Cognitive emissions of $1/f$ noise. *Psychol Rev* 98:554–568
- Keele SW (1968) Motor control in skilled motor performance. *Psychol Bull* 70:387–403
- Keele SW, Posner MI (1968) Processing of visual feedback in rapid movements. *J Exp Psychol* 77:155–158
- Khan MA, Franks IM, Elliott D, Lawrence GP, Chua R, Bernier PM, Hansen S, Weeks DJ (2006) Inferring online and offline processing of visual feedback in target directed movements from kinematic data. *Neurosci Biobehav Rev* 30:1106–1121
- Meyer DE, Abrams RA, Kornblum S, Wright CE, Smith JEK (1988) Optimality in human motor performance: ideal control of rapid aimed movements. *Psychol Rev* 95:340–370
- Miyazaki M, Kadota H, Kudo K, Masani K, Ohtsuki T (2001) Fractal correlation of initial trajectory dynamics vanishes at the movement end point in human rapid goal-directed movements. *Neurosci Lett* 304:173–176
- Miyazaki M, Nakajima Y, Kadota H, Chitose K, Ohtsuki T, Kudo K (2004) $1/f$ -type fluctuation in human visuomotor transformation. *NeuroReport* 7:1133–1136
- Peng CK, Havlin S, Stanley HE, Goldberger AL (1995) Quantification of scaling exponents and crossover phenomena in nonstationary heartbeat time series. *Chaos* 5:82–87
- Slifkin AB, Eder JR (2012) Amplitude requirements, visual information, and the spatial structure of movement. *Exp Brain Res* 220:297–310
- Slifkin AB, Grilli SM (2006) Aiming for the future: prospective action difficulty, prescribed difficulty, and Fitts Law. *Exp Brain Res* 174:746–753
- Valdez AB, Amazeen EL (2008) Using $1/f$ noise to examine planning and control in a discrete aiming task. *Exp Brain Res* 187:303–319
- Valdez AB, Amazeen EL (2009) Target dimension affects $1/f$ noise in aiming. *Nonlinear Dyn Psychol Life Sci* 13:392–396
- van Beers RJ (2009) Motor learning is optimally tuned to the properties of motor noise. *Neuron* 63:406–417
- van Beers RJ, Brenner E, Smeets BJ (2013) Random walk of motor planning in task-irrelevant dimensions. *J Neurophysiol* 109:969–977
- Wijnants ML, Cox RFA, Hasselman F, Bosman AMT, Van Orden G (2012) A trade-off study revealing nested timescales of constraints. *Front Physiol* 3:1–15
- Wing A, Daffertshofer A, Pressing J (2005) Multiple time scales in serial production of force: a tutorial on power spectral analysis of motor variability. *Hum Mov Sci* 23:569–590